An Improved Visualization of Diesel Particulate Filter

by

Kevin Boehm

Submitted to the Department of Mechanical Engineering in Partial Fulfillment of the Requirements of the Degree of

BACHELORS OF SCIENCE IN MECHANICAL ENGINEERING

AT THE

MASSACHUSETTS INSTITUTE OF TECHNOLOGY

June 2011

Signature of Author: _____

Department of Mechanical Engineering
April 29, 2011

Certified by: _____

Thomas W. Eagar
Professor of Material Science Engineering and Engineering Systems
Thesis Supervisor

Accepted by: _____

John H. Lienhard V
Samuel C. Collins Professor of Mechanical Engineering
Undergraduate Officer

(This page intentionally left blank)

An Improved Visualization of Diesel Particulate Filter

by

Kevin Boehm

Submitted to the Department of Mechanical Engineering in Partial Fulfillment of the Requirements of the Degree of

BACHELORS OF SCIENCE IN MECHANICAL ENGINEERING

ABSTRACT

The prevalence of diesel particulate filters (DPF) is increasing as emissions standards worldwide evolve to match current technologies. Since the first application of DPFs in the 1980's, PM trapping effectiveness has increased by orders of magnitude. During the filter's use phase, it is subject to multiple cycles of particulate matter trapping and regeneration. The soot particles are combusted in the high temperatures; however, metal additives referred to as ash, primarily from lubricants, remain behind and restrict exhaust flow. Further ash accumulation causes a pressure drop across the filter and necessitates replacement in order to maintain fuel economy and engine performance.

Research into more efficient DPF designs and geometries examines current limitations with the goal of emitting cleaning emissions and extending DPF use. In order to gain a better understanding of PM trapping and regeneration and acquire real-time feedback, an improved visualization method of DPF is required. For that method, powder glass frit was applied between the filter and glass window and heated to form a bond. After the heating process, the bond strength was measured to determine optimal heating cycles and surface conditions for the glass seal.

The experimental results were examined to measure the success of the bonding method relative to previous research using alternative methods. The ability to test and observe ash accumulation in different DPF designs will contribute to the understanding of PM trapping.

Thesis Supervisor: Thomas W. Eagar
Title: Professor of Material Science Engineering and Engineering Systems

(This page intentionally left blank)

ACKNOWLEDGEMENTS

I would like to thank some of the people who have helped make my time at MIT so valuable. The four year journey has been extremely challenging, but my experiences inside and outside of the classroom have taught me more than I ever imagined.

I am very thankful to Dr. Thomas Eagar for his all his help and advice over the past few years. The ability to work on problems and learn material outside of my undergraduate curriculum has been beneficial to my academic development. Additionally the resources available to me in the MIT Welding and Joining Laboratory have been indispensable. Additionally, I would like to thank Dr. Harold Larson, Donald Galler, and Brian Hohmann for all of their help in the lab and with my thesis.

I would also like to thank Iason Dimou for presenting me with the problem that led to the development of the hypothesis and methods.

Furthermore, I would like to thank all of my friends who have been with me during some of my best and worst times at MIT.

Most of all I would like to thank my family for everything they have done over the years to prepare me for school, and more importantly, my future. Their unwavering support has guided me along and been integral to my path to graduation. Finally, I would like to thank my girlfriend Mary for motivting me and making my last year at MIT the most memorable.

(This page intentionally left blank)

TABLE OF CONTENTS

LIST OF FIGURES

LIST OF TABLES

NOMENCLATURE

Ca	Calcium
CDPF	Catalyzed Diesel Particulate Filter
DPF	Diesel Particulate Filter
EPA	Environmental Protection Agency
Mg	Magnesium
NO_x	Nitrogen Oxide
PM	Particulate Matter
SiC	Silicon Carbide
SiO_2	Silicon Dioxide
Zn	Zinc

1 INTRODUCTION

In diesel engines, exhaust emissions pass through a Diesel Particulate Filter (DPF) before entering the atmosphere. The DPF effectively filters greater than 90 percent of particulate matter (PM) [1]. During operation, the filter progressively clogs with both soot and ash. The soot is burnt off during regeneration cycles where the filter is heated, combusting the carbon soot into either carbon dioxide or carbon monoxide.

The residual ash remains after regeneration and continues blocking the filter channels. Ash accumulation diminishes performance and ultimately requires a new replacement filter. The ability to examine different DPF geometries and configurations during PM trapping and regeneration can increase the knowledge base on PM trapping and lead to improved production of more efficient filters.

1.1 Diesel Particulate Filter

Most DPFs are ceramic wall flow filters, although there are other less common material options including ceramic fibers and sintered metals. DPF's were first used by Mercedes Benz in 1985 and became popular in the 1990's retrofit market for machinery, mining equipment, and heavy duty vehicles. Because of government regulations that limited PM emissions to 10-20% of prior standards in the United States, Europe and Asia, DPF usage for automobiles greatly increased in the 2000's [1].

Wall flow DPFs are produced with different materials and geometries, but in principle use the same method to filter PM. On the entry side, every other square-shaped cell entrance is plugged, and the exit portion of the open flows cells are plugged. As illustrated in Figure 1.1, the flow pattern forces the emissions to enter the open cells, pass through a cell wall, and exit the open cells. As a result, soot and ash PM accumulates along the boundary where the emissions flow transitions between cell channels.

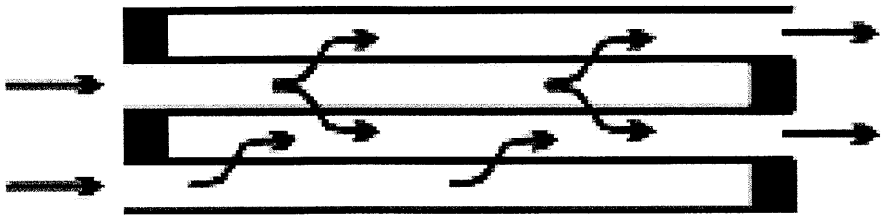

Figure 1.1. Illustration of exhaust flow through wall-flow DPF [1].

1.1.1 DPF Materials

Beyond filtering capabilities, DPF materials must have a high maximum operating temperature, low thermal expansion coefficient, and chemical resistance to diesel emissions. Because of the application in automobiles, filter materials ideally are also low cost and low density. The most common material selections are ceramics such as cordierite, $2MgO\text{-}2Al_2O_3\text{-}5SiO_2$, and silicon carbide, SiC [1].

A comparison can be drawn between DPFs and catalytic converters, which are commonly used in conventional spark ignition (SI) engines, because of similarities in the honeycomb filter appearance. Unlike DPFs, where the emissions are forced through the pores of the wall, catalytic converters passively convert emissions into less harmful substances. Because the particulate matter is not trapped, catalytic converters have completely open cells. While the material porosity of DPFs is tightly controlled for effectiveness, catalytic converters simply expose the emissions to the metal catalyst, which is often platinum.

Some DPFs, appropriately named catalyzed diesel particulate filters, CDPFs, contain a catalyst material, like catalytic converters, to increase filtering capabilities. With the addition of a catalyst, the CDPF enhances typical PM trapping by enabling oxidation of

PM prior to regeneration heat cycles. Table 1.1 lists typical size ranges of filter geometries for cordierite and silicon carbide DPFs.

Property		Cordierite	SiC
Channel Width	(mm)	1.3-2.1	1.0-1.6
Wall Thickness	(mm)	0.3-0.5	0.3-0.8
Mean Pore Size	(μm)	13-34	8-17
Porosity	(%)	45-50	42-58
Permeability	(m^2)	$0.5 - 10^{-12}$	$1.2 - 1.3 \times 10^{-12}$
Melting/Sublimation Temperature	(°C)	1,450	1,800-2,400

Table 1.1. Average range of properties for cordierite and silicon carbide DPFs [2].

1.1.2 Pressure Drop

As the DPF channels trap carbon soot and ash, pressure across the filter drops and degrades engine performance. Specifically, the accumulation of soot and ash reduces the hydraulic diameter and channel length. At the beginning of a DPF use phase, the material trapping occurs in the pores of the filter along the transition between channels. Eventually the distance from the emissions entry to the wall transition point decreases and particulate matter begins accumulating along the filter walls. The total pressure drop is calculated by adding the components of different pressure drops as the following:

$$\Delta P_{total} = \Delta P_{in} + \Delta P_{out} + \Delta P_{channel} + \Delta P_{wall} + \Delta P_{ash} + \Delta P_{soot} \quad (1.1)$$

The pressure drops at the entrance and exit of the filter are functions of the filter entrance and exit areas, respectively, and make up a small part of the total pressure drop. Assuming laminar flow, the pressure drop due to frictional losses along the channel is equal to:

$$\Delta P_{channel} = 4f\left(\frac{L}{D_h}\right)\left(\frac{\rho v^2}{2}\right) \tag{1.2}$$

Where f is the friction factor, L is the channel length, ρ is the exhaust density, and v is the exhaust velocity. D_H is the hydraulic diameter which is equal to:

$$D_H = \frac{4A_S}{P} \tag{1.3}$$

where A_s is the surface area and P is the wetted perimeter. The friction factor is calculated using the correlation for laminar flow through a square channel, in which K equals 14.23, and where:

$$f = \frac{K}{Re} = \frac{K}{\frac{\rho v D_H}{\mu}} \tag{1.4}$$

The pressure drop caused by the friction in the channel is initially much smaller in magnitude than the pressure drop caused by trapping in filter pores. To calculate the pressure drop of the material in the pores, a simplification of Darcy's pressure drop law yields:

$$\Delta P_{wall} = \Delta P_{ash} = \Delta P_{soot} = \frac{\mu}{K_P} \cdot v_w \cdot w \tag{1.5}$$

In equation 1.5, μ is the exhaust gas viscosity, K_p is the material permeability, v_w is velocity along the wall, and w is the thickness of the material layer. During accumulation, the pressure drop increases because the material permeability decreases and thickness of the material layer increases. Because of the different forms of accumulation and factors affecting the total pressure drop, the pressure drop rate of change varies with time.

The rate of change of pressure drop is the highest during the initial mode of trapping before the pores in the filter are filled with PM, and it eventually reaches a steady state

value. Figure 1.2 shows the effect of channel restriction from accumulation on pressure drop up until complete channel area restriction.

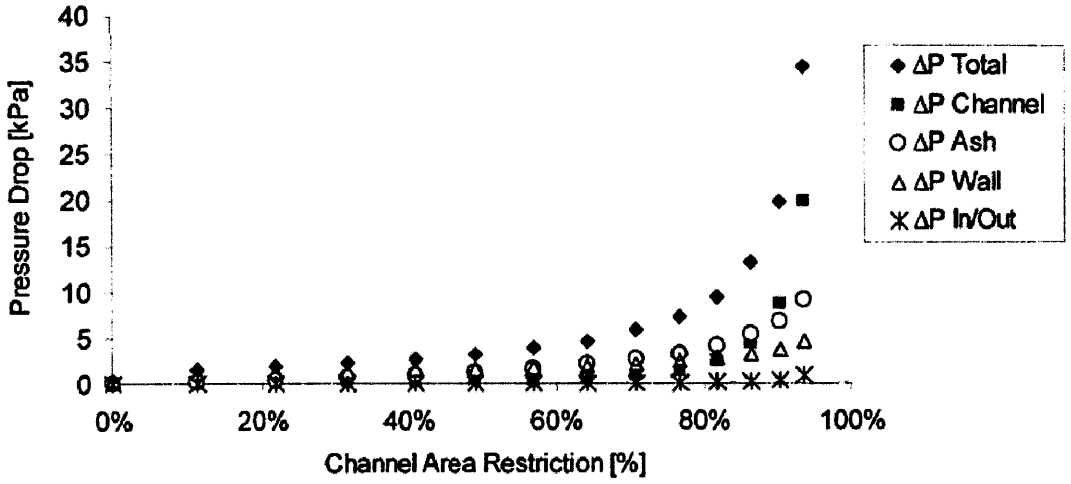

Figure 1.2. Development of pressure drop for components of total pressure drop during ash accumulation on channel walls [2].

1.2 Diesel Emissions

Combustion of diesel fuel releases CO_2, H_2O, O_2, and N_2, as well as regulated emissions including CO, hydrocarbons, particulate matter, and nitrogen oxides (NO_x). Compared to SI, diesel or compression ignition (CI) engines reduce CO and hydrocarbon emissions, but produces significantly more NO_x and PM [1]. The differences in emissions, illustrated in Figure 1.3, shows the cost benefit analysis of the CI system over SI.

According the United States Environmental Protection Agency (EPA), more than one third of the US population lives in areas where particulate matter exceeds the established air quality limits. In addition, the EPA currently recognizes diesel particle emissions as a carcinogen and factor for respiratory illness and heart attacks [3]. Therefore, improving

DPF efficiency and decreasing regulated emissions would have a positive impact on both people and the environment.

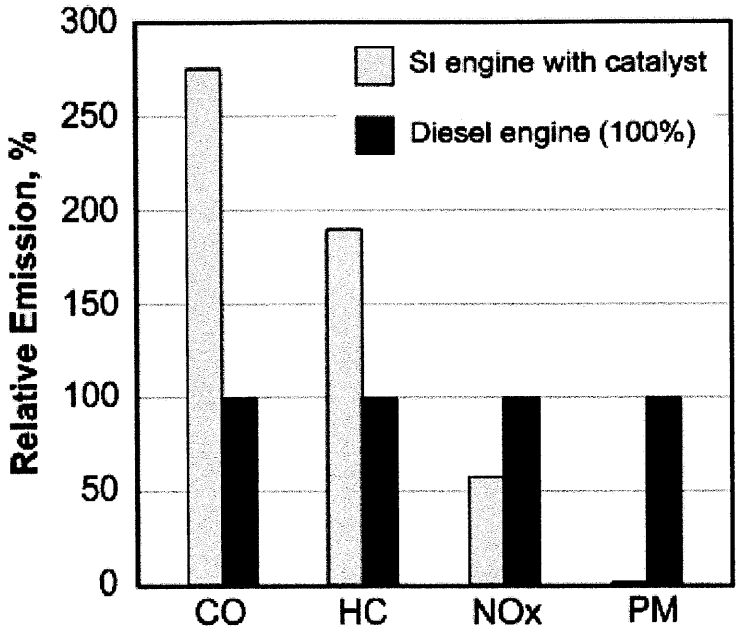

Figure 1.3. Comparison of emissions of spark ignition, SI, to emissions of diesel Engines, using 4-cylinder 1.7L MY1992 engine. The results, which are normalized to the diesel engine, indicate carbon monoxide, hydrocarbon, nitrogen oxides, and particulate matter emissions [1].

1.2.1 Soot and DPF Regeneration

Soot, the combustible portion of the emitted PM, accumulates in the pores and along the walls of the filter. The soot emitted from the diesel engine is primarily composed of black carbon particles, the second largest contributor to global warming [2]. Because it is a combustible particulate, the soot can be burned out of the filter in order to decrease the pressure drop and improve system performance. The percentage of soot in PM varies based on the engine and operating conditions.

DPF regeneration, the process of burning soot off the filter, begins at temperatures above 360°C and occurs quickly and completely at temperatures above 600°C [1]. The products

of regeneration are affected by how much oxygen is available during combustion; specifically, oxygen deprivation leads to CO production instead of CO_2. While soot is relevant for its CO_2 and global warming potential, the fact that it can be easily removed from the filter, compared to ash, makes it less of a focus for DPF development. Figure 1.4 details the DPF temperature and pressure changes during a series of regeneration processes that remove soot and restore DPF and system performance. Over the life of a DPF, increased pressure drop and sensitivity to soot lead to an increased frequency of regeneration cycles.

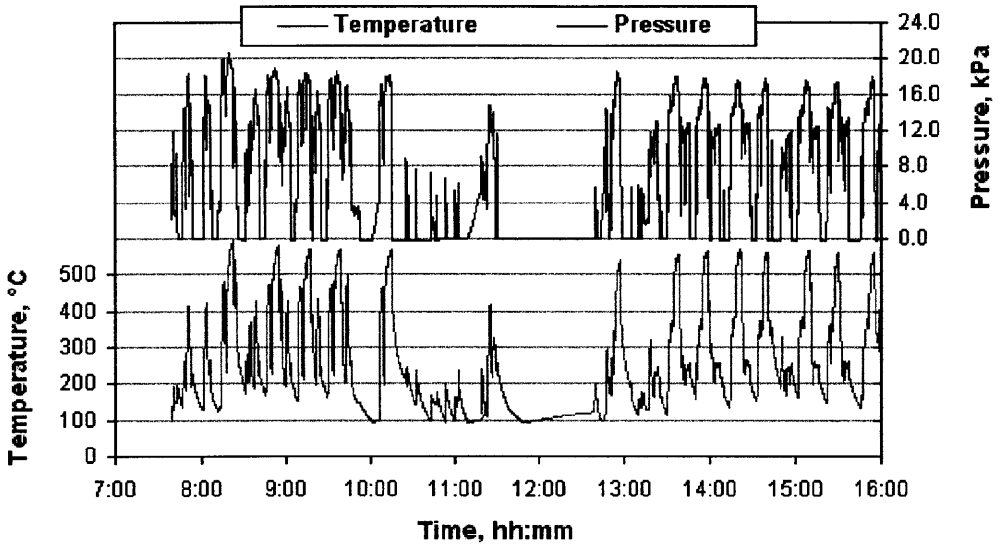

Figure 1.4. Pressure and temperature of DPF over a series of regenerations [1].

1.2.2 Ash Properties and Accumulation

The burning of engine oil additives, metal impurities from engine wear, and corrosion of the exhaust system contribute to the metallic ash in diesel emissions. However, the majority of the ash is composed of engine oil additives, giving it a makeup of sulfates, phosphates, Ca, Zn, and Mg oxides [1].

The quantity of ash within the DPF increases as it accumulates; however, the modes of accumulation and resulting pressure drops vary with ash concentration. During the early periods of PM trapping, ash and soot are evenly distributed along the channel surface. After periodic regenerations remove the soot, a plug of ash forms at the end of the channel before the forced transition into an open cell. With continued PM trapping and regenerations, this plug increases in length and restricts exhaust flow.

Over the use phase of the DPF, ash blockages make up an increasingly larger proportion of solid PM. Specifically, the ash accounts for more than half of the PM after more than 33,000 miles of service. After 150,000 miles, the EPA mandated time of service, ash makes up more than 80% of the PM [4]. The amount of ash particulate matter, therefore, is the critical quantity, and any modifications that decrease PM trapping's pressure drop will lead to a longer DPF life cycle.

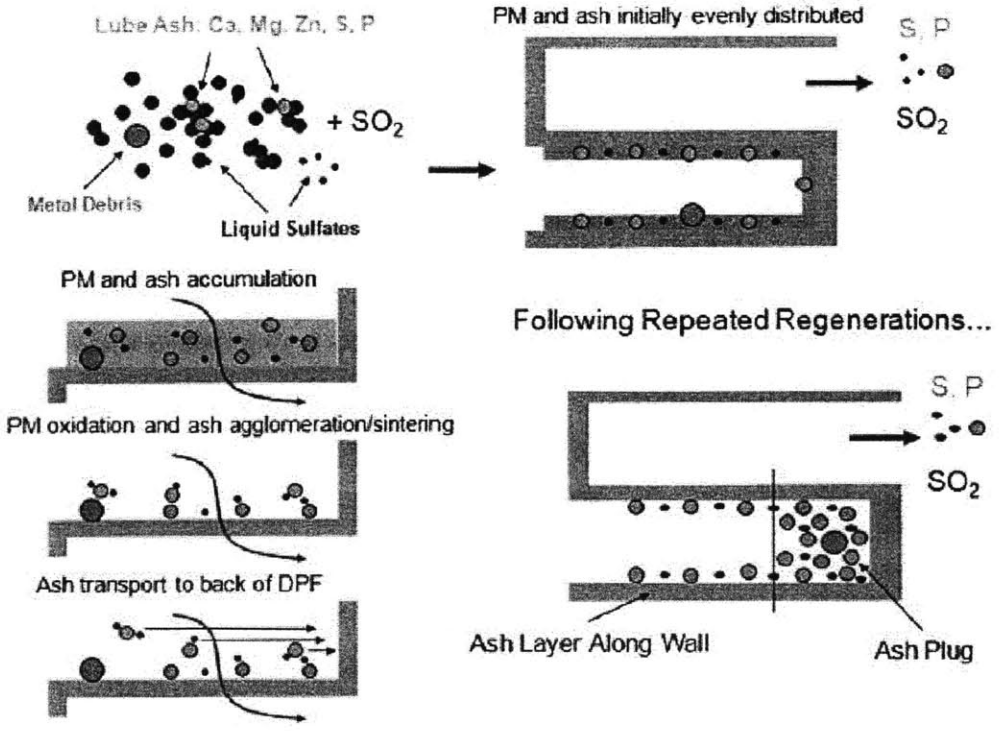

Figure 1.5. Development of ash plug during PM trapping and regeneration. Over time the ash plug progressively moves along the channel length [2].

1.3 DPF Bonding

Visualization methods that enable a real time view of emissions in the DPF help improve the understanding and modeling of PM trapping and regeneration. Previous methods have accomplished such a visualization for a small DPF area two channels wide, of dimensions 8mm width and 15mm length [5]. The method provided a view of a horizontal slice, showing the emissions flow through the two open channels to the end of the closed cell where the ash plug formation begins. In order to improve the visualization, a larger area and all the top layer channels, including those with initially closed cells, will be examined.

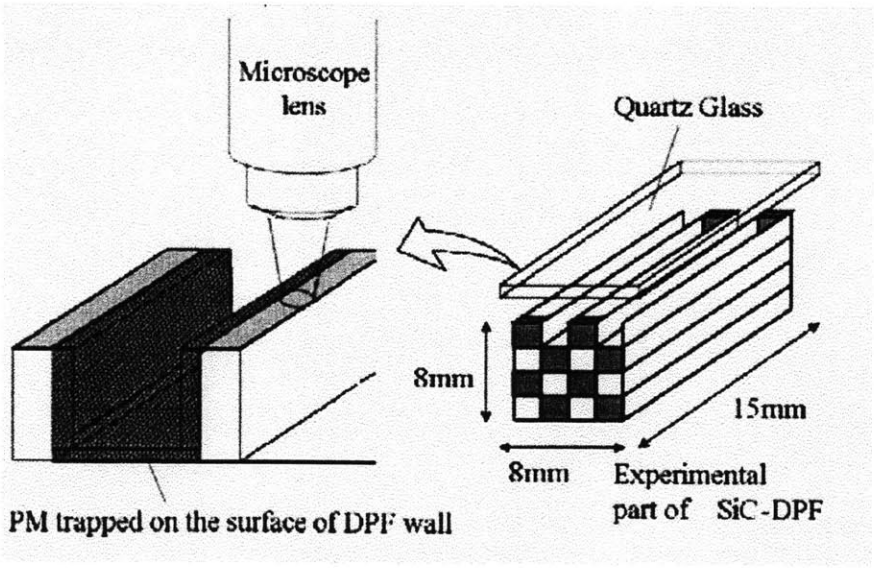

Figure 1.6. Visualization and scale of previous DPF viewing methods for small size areas [5].

1.3.1 Frit Bonding Method

The proposed improved visualization method differs from previous methods in that it examines a larger area of filter channels with less surface area to bond. Because all the channels, not every other, will be open for visualization, only the filter surface between the walls will remain available for bonding. Glass frit, a very fine powder, will be

applied to the filter surface area and bonded to a glass surface in hopes of establishing an airtight seal. When heated in a furnace, the frit will wet and bond the surfaces if prepared correctly, similar to metallic soldering methods.

1.4 Objectives

Based on previous methods of DPF visualization and data presented in the literature, a working improved visualization method utilizing glass frit bonding would yield relevant data for PM trapping and regeneration. If applied to multiple filter materials, sizes, and geometries, the visualization method could be used to obtain complete data sets for all varieties of diesel particulate filters. If the method is not completely successful, the working features will be recognized for use in future methods, and the failing features will be examined for cause of failure.

Methods that improve the quantity and quality of data available for DPF emissions are crucial for the development of more efficient filters. Ultimately, any improvements in diesel efficiencies and standards lead to lower PM and CO_2 output. Given the widespread usage of diesel engines in manufacturing, transportation, and industrial applications both in the US and worldwide, better DPFs can lower the amount of harmful airborne PM and reduce global warming potential on a large scale.

2 TEST SETUP AND EXPERIMENTAL PROCEDURE

All of the diesel particulate samples examined in the testing were new and unused sections. Each sample was extracted and prepared for optimal bonding conditions in order to attempt assembly of the improved visualization method. The samples were prepared sections of rectangular filter segments and were heated in a furnace in order to attempt bonding with a glass surface. Because of the DPF application in an engine cycle, the range of operating temperatures, as well as regeneration process temperatures, drives the materials selection process.

The samples were heated inside a box furnace with the temperature monitored by a digital thermometer connected to a type-k thermocouple. The samples were elevated on a brick surface and positioned in the rear section of the furnace near the thermocouple in order to maximize the temperature reading accuracy.

After undergoing a heating cycle the bond strength, if applicable, was tested in order to examine the consistency of the seal. Ideally the bond will be airtight and prevent the escape of any diesel emissions, as well as particulate matter. However, some inconsistencies in the bonding surface can be tolerated and may still be capable of yielding results because soot and ash will eventually clog any openings.

Throughout the experimental process, different test assemblies and procedures were tested, and the results of each were compared. The methods that enable the strongest and most consistent bonds will be further examined for their application in a larger test setup. The ultimate goal of the bonding process is to be able to examine a large area, on the order of the size of the filter, as opposed to the size of a few cells. Given a working method on the smaller order, the method should be capable of being scaled to achieve this larger viewing area.

2.1 Important Parameters

The most important factor of the bonding process is the temperature, specifically the cycle of temperatures applied during the heating phase. Not only will the temperature change be controlled and examined from trial to trial, but the heating/cooling rates and process times will also be varied to examine their effects. The heating boundary conditions are determined by materials and the filter regeneration process. As a result, the glass viewing window must be capable of withstanding temperatures of up to 700°C [1]. After its use in the test setup, during which it is exposed to heated emissions, the glass will be highly susceptible to cracking during the cooling phase. However, the area

of interest is the DPF during the use phase, so the integrity of the surface is only critical during PM trapping and regeneration .

Heating cycle data was based on and adapted from glass manufacturer recommendations and product descriptions. Important stages in the heating cycle include initial heating, process soak, annealing, and cooling. Variations in the heating and cooling will dictate whether the frit structure is crystalline or amorphous. Because microscopic, and even macroscopic, observation requires transparency, formation of a crystalline structure is essential.

Step	Rate (DPH)	Temperature (°C)	Hold (min)
1. Initial Heat / Process Soak	400	720	10
2. Rapid Cool / Anneal Soak	AFAP	480	30
3. Final Cool	AFAP	20	0

Table 2.1. The three step heating cycle where the temperature is heated to the melting point of frit, annealed, and cooled. AFAP indicates a cooling rate of "as fast as possible."

Step	Rate (DPH)	Temperature (°C)	Hold (min)
1. Initial Heat / Process Soak	400	720	10
2. Rapid Cool / Anneal Soak	AFAP	480	30
3. Anneal Cool	100	370	0
4. Final Cool	AFAP	20	0

Table 2.2. The same process as the first heating method, with the addition of an annealing cooling step from 480-370°C.

Step	Rate (DPH)	Temperature (°C)	Hold (min)
1. Initial Heat / Process Soak	400	720	30
2. Rapid Cool / Anneal Soak	AFAP	480	30
3. Anneal Cool	100	370	0
4. Final Cool	AFAP	20	0

Table 2.3. Heating cycle with an extended process soak time period

The three different heating and cooling cycles vary in the length of time for the process soak (10 minutes for 2.1 and 2.2, 30 minutes for 2.3) as well as the addition of the annealing process in 2.2 and 2.3. Annealing, which is a slower cooling rate from the heating process temperature, relieves the internal stress within the glass surface. As a result, the visualization window is stronger and less likely to crack from temperature change or mechanical strain.

2.2 Sample Preparation

The filter sections were prepared for bonding by establishing a flat plane in order to maximize contact area with the glass. Initially a rectangular section of DPF was removed from the array of sections in a full size filter. This section was then cut into smaller pieces, ranging in width from 5 to 24 cells (or 7.6 to 35.0mm). All of the DPF samples were composed of silicon carbide (SiC), which has a low coefficient of thermal expansion and high hardness. To sand the filter, a tool with a larger surface hardness is required. Therefore, a diamond wheel cutting tool was used to planarize the surface.

Three different surface profiles were prepared for bonding experiments, ranging in surface area. Surface type A, depicted in Figure 2.2 is a completely flat surface with no channel openings and is the easiest surface to bond. Figure 2.2 shows type B, which has

every other channel top surface sanded open. Finally, the most difficult surface, type C, has only the walls between each channel remaining.

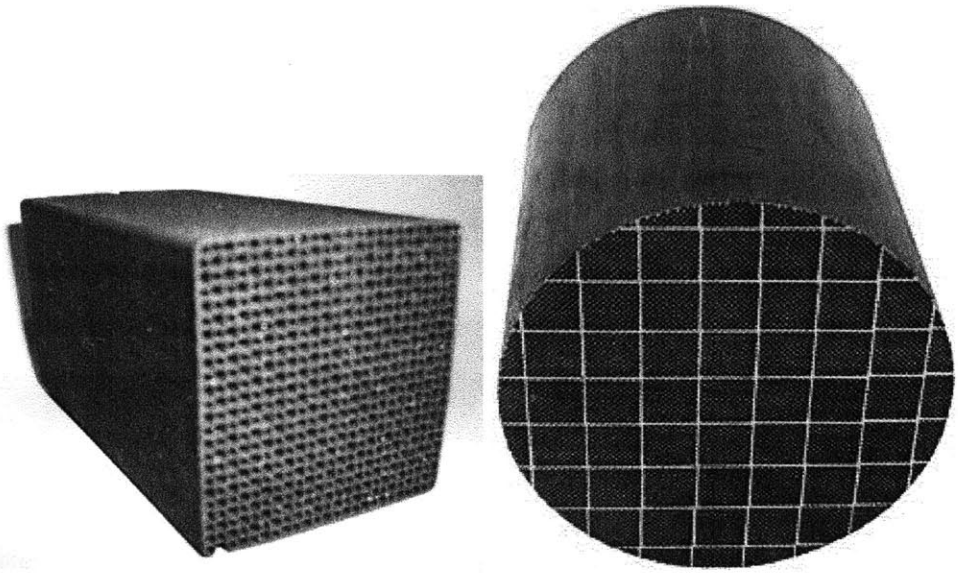

Figure 2.1. Visualization and scale of previous DPF viewing methods for small areas [1].

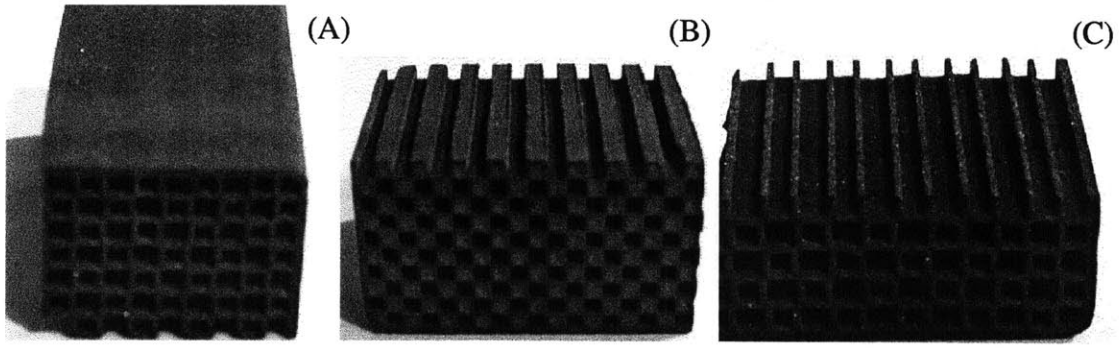

Figure 2.2. From left to right, surface types A, B, and C, used for different trails of surface bonding.

Regardless of the surface type, the same method is followed for bonding. Similar to the soldering process, the surfaces are wetted when the bonding medium reaches a high enough temperature to flow. Instead of a lead-tin solder, powder glass frit was applied to both the glass and the silicon carbide filter.

The glass viewing surface must be able to withstand the temperatures in the test setup. Previous experiments have used fused quartz glass as the material of choice due to its strength and high melting point [5]. A proposed acceptable material choice instead of fused quartz is Vycor, a material that is 94% SiO_2, 5% B_2O_3, and 1% Na_2O [6].

The glass frit is added to the surface of the fused quartz or Vycor for bonding by applying a paste of petroleum jelly and powdered glass frit. In the kiln the petroleum jelly burns off at a much lower temperature than the softening temperature of the glass. As a result, the frit is held in place until it reaches a temperature sufficient to wet and bond to the surface. Initial testing to verify the frit wetting properties on both the fused quartz and the DPF entailed the heating of frit on each surface individually and examination of the cooled frit surface contact angle.

Given the proper heating cycle, amount of powder frit, and pressure on the bonding surfaces, the two surfaces should tack bond and adhere to one another. Once initial testing of material properties and proof of concept is complete, an optimal heating cycle was be selected, and bonding results for each surface type were examined. The results should yield a representation of the capabilities and consistency of the visualization method, and its potential application for a study of DPF trapping and regeneration.

3 RESULTS

In the experiment, the apparatus/method was setup in order to demonstrate proof of concept for the frit bonding method. Repeated trials and their results helped determine which surface area types and heating/cooling cycles were optimal for the tack fusing process. The results ranged from hopeful to successful to failure. An examination of the causes of success or failure is essential to development of new methods in future work. Furthermore, additional research into the causes of success or failure increases the understanding of DPF bonding and ultimately PM trapping and regeneration.

3.1 Surface Bonding

The magnitude of success in bonding to each surface, as one would expect, was proportional to the available surface area for bonding. Other factors, including the amount of powder glass frit applied and the consistency of the DPF terrain, also determined the bonding success. The dimensions of the sample, specifically for the larger samples, amplified any imperfections in the surface. Additionally, the more complex surface area types required more sample preparation and attention to establish a consistently flat plane, increasing the probability of failure. The fact that only surface types B and C, where open channel area is exposed, provide an improved visualization of the DPF does not trivialize the results for surface type A. Instead, the observations of the bonding to the flat plane provide a benchmark for comparing bond structure and strength to the other samples.

3.1.1 Surface Type A

As expected, the bonding to the consistent flat plane surface was the most successful of the three surface types. Figure 3.1 displays the sample after firing and bonding, demonstrating where the tack bonding is large enough to secure the glass surface to the silicon carbide filter. The test was repeated in several trials at the optimum temperature

cycle with varying concentrations of frit, as shown in Figure 3.2. As the amount of frit increased per trial the strength of the bond increased, but at the expense of visibility. For the fired sample in Figure 3.1, the largest amount of frit displayed in Figure 3.2 was used for bonding. The samples with more secure bonds were prepared with flatter, more consistent surfaces.

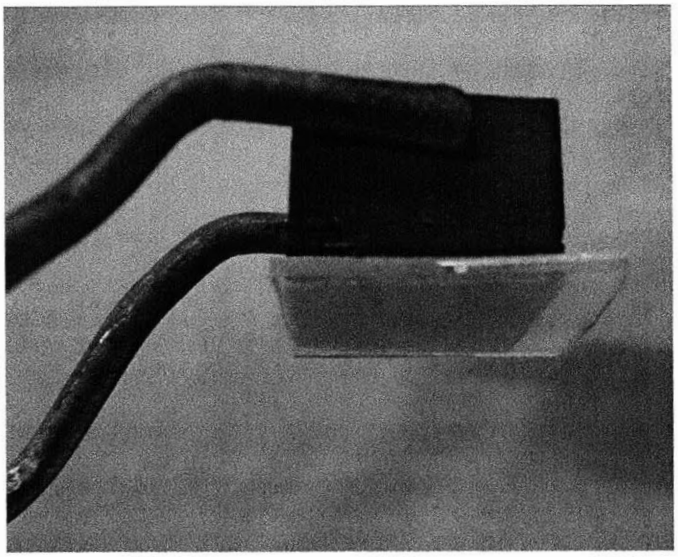

Figure 3.1. Surface type A bonded to fused quartz, withstanding the force of gravity.

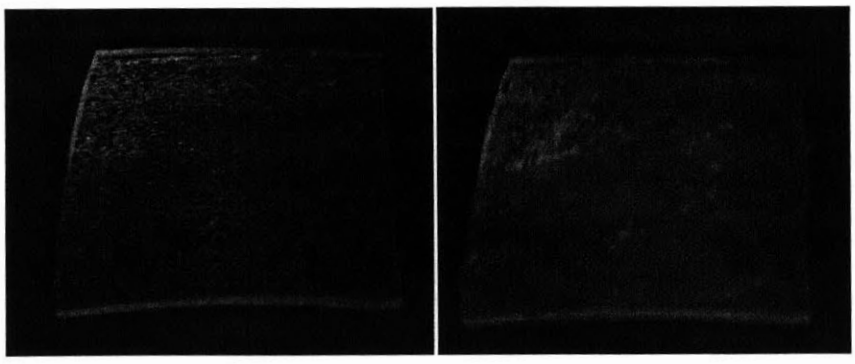

Figure 3.2. Comparison of frit applied to glass surface for bonding attempts. The contrast of the images is amplified proportionally for both images in order to illustrate the increased frit concentration for the second image.

The failure of the glass to filter bond occurred when the glass was forced upwards, away from the DPF surface. The force required to separate the bond is small, on the order of 10 Newtons; however, it is sufficient for the application in a diesel emissions test setup. The more critical failure mode occurs when the glass, or DPF, is rotated relative to the other surface. The magnitude of force required to shear the bond is much smaller than that required to pull the bond apart axially. Additionally, it is more likely that the sample will be hit in this manner while being mounted into a test setup.

Another important factor about the bonding to surface type A is that the flat filter surface can maintain a much higher load and overall pressure than the other surface types. A significant amount of force, much less than what is needed during the bonding process, is required to buckle the filter surface.

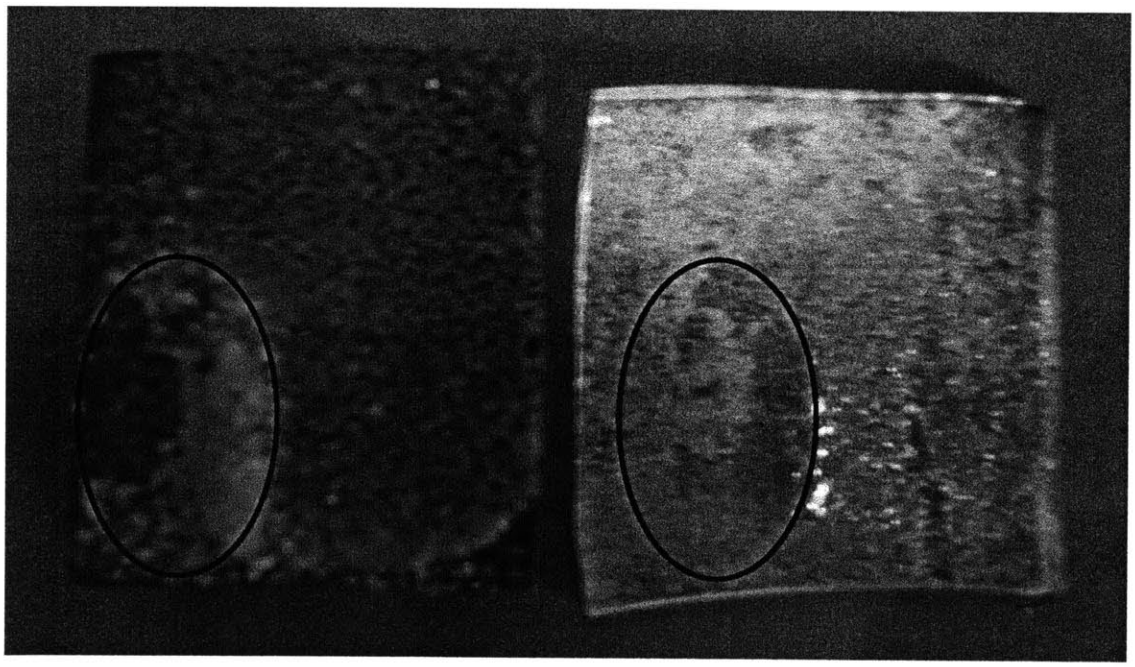

Figure 3.3. Filter and glass surface after axial mode of failure. The indicated areas of interest, in the same location of each surface, show the transfer of frit to the DPF.

Examination of the bond failure of the strongest sample enables an understanding of the method weaknesses. As shown in Figure 3.3, the bond failure occurs differently across the surface of the two materials. The indicated area of interest displays two regions, one on the filter surface where a large amount of frit accumulated and another on the glass where all the frit has been removed. This irregularity was likely caused by insufficient wetting of the frit particles.

3.1.2 Surface Type B

Because of the removal of half the channels, the available surface area for bonding on surface type B is half of the available area for type A. The same bonding process previously described and used for surface type A proved ineffective in joining surface type B to the glass. Repeated trials using the method, in which petroleum jelly and then glass frit is first applied to the glass, yielded no successful results for any of the temperature cycles.

The frit application method for surface type B was adapted to initially apply the frit to the filter surface. Similar to the previous method, a thin layer of petroleum jelly was applied to the top surface on all the raised channels, and then the frit was applied to the filter. Additionally, the open channel areas were wiped clean in order to clear out any frit material that could potentially block the flow area. Figure 3.4 shows the prepared surface type B before bonding. In contrast to the originally prepared surface, as depicted in Figure 2.2 (B), the layer of glass frit covers the DPF top area.

Multiple filter surfaces were prepared following this adapted procedure, with two variations of the bonding process. Initially, the DPF frit application method was tested by preparing the surface and heating through a complete cycle without bonding the top glass layer. Similar to wetting a metal surface with solder, the DPF became coated with the glass as it softened and hardened in the furnace. Whether the material was prepared

in this manner where the pre-wetted surface is reheated with the fused quartz layer, or both surfaces are wetted and bonded in the same step, the bonding strengths were the same.

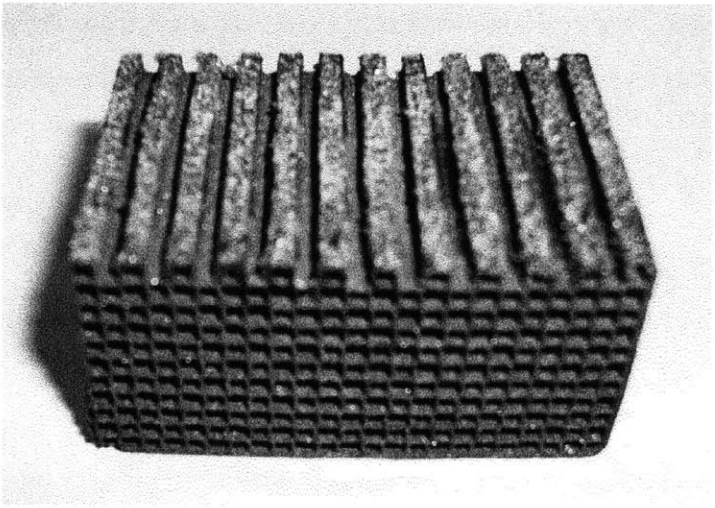

Figure 3.4. The bonding surface of surface type B following the DPF frit wetting procedure and subsequent heating.

As for the flat plane with no channels removed, surface type B bonded best to the glass surface when liberally applied with glass frit. An important factor to consider is that establishing bond strength was a much higher priority than visibility through the glass surface. Once a methodology for surface bonding is established, parameters such as the heating cycle and frit properties can be adjusted to improve the visualization of the filter surface.

The most successful bonding attempts with surface type B occurred when the surface area, or number of channels, was minimized. For the sample displayed in figure 3.5, the surface area was reduced by a width of 8 cells. As a result, there were 4 full channel surfaces and one outer channel was available for bonding sites.

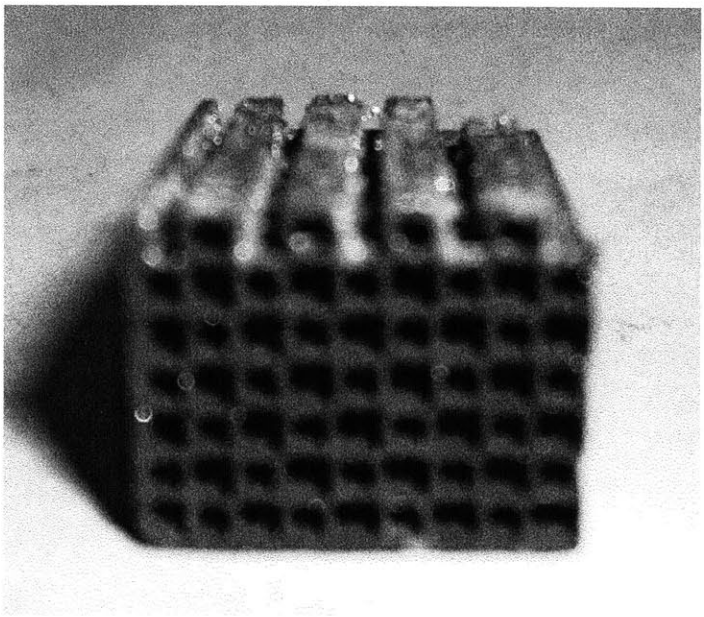

Figure 3.5. Surface type B wetted with powder frit after heating and cooling cycle.

The sample displayed in Figure 3.5 is the result of a surface bonding process and axial failure mode separating the filter from the glass. Due to the reduced surface area from surface type A, the bond strength and resulting force necessary to break the bond is much smaller, requiring approximately one order of magnitude less force. The difference in strength is not limited by the bond strength between the frit and the glass or filter, but instead by the lower force required to fracture the filter surface. Figure 3.6 shows the portions of two filter cells removed from the DPF surface and bonded to the glass.

Given the eventual DPF visualization test setup, the axial separation force will be limited, and instead the bond area of the viewing windows will be pressurized by the holding fixture. As a result, the critical failure mode, other than rotational surface shearing of the frit bonding or the filter surface from itself, is the compressibility of the filter. If the

channel surfaces are crushed under the pressure of the test fixture, the seal will be broken, and the sample will be rendered useless.

In order to maintain the necessary pressure for bonding, the applied compression force on the surface must increase as the surface area itself increases. As a result, any raised areas, even just slightly above the intended plane height, will be subject to increasingly high forces and ultimately buckle.

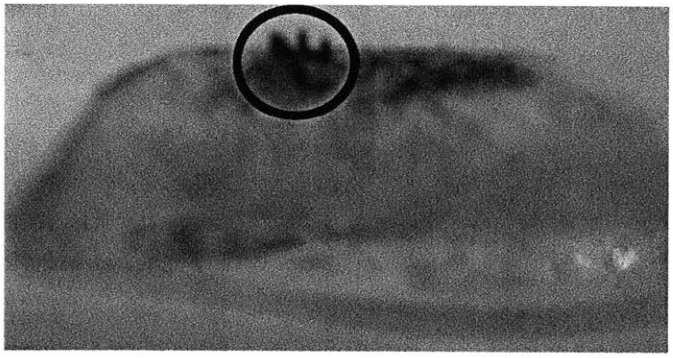

Figure 3.6. The section of DPF channels removed from minimal axial separation force between the filter and glass surface, indicating that the frit bond strength is greater than the silicon carbide critical axial stress.

3.1.3 Surface Type C

The ultimate goal of the improved visualization method was to establish a bond with only the channel wall, allowing visibility in every channel along the top surface. However, the difficulties in bonding surface type B were magnified as the surface area was decreased even further for surface type C. The removal of the top surface reduced the available bonding surface area by a factor of three approximately.

Given the smaller surface area, application of frit by any method was increasingly difficult. A large enough amount of frit for bonding could not be applied directly to the DPF, as was done for surface type B, so a modified version of the original application method to the glass was performed. In order to test whether bonding to this small of a

surface was possible, larger amounts of frit were added to the glass surface in each trial until the entire glass surface was covered by a thin film. It is important to note that the function of a visualization window at this point is deficient because of all the frit; however, the emphasis of testing was to test the feasibility of bonding to this surface type.

Therefore, bonding for this surface with the frit method, or any method requiring compression of the channel walls, is hindered by the brittle nature of the filter. When there are two or more walls connected to the top surface, as in surface types A and B, the compressive force on one wall is counteracted by the tension force on the connected walls, as shown in Figure 3.7. When there is no wall connecting the surfaces, as in surface type C, any deflection alters the compressive force direction into that of a shear force, resulting in surface fracture.

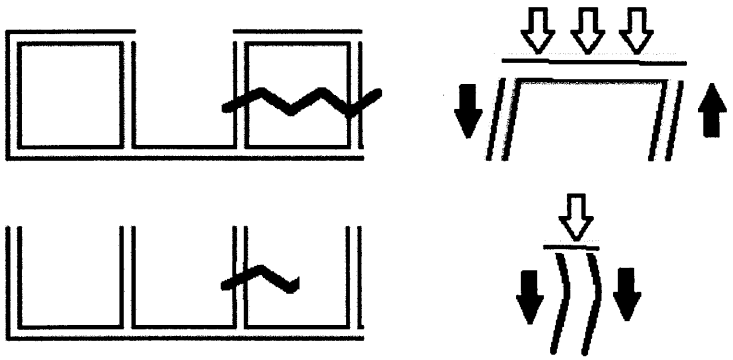

Figure 3.7. In the force diagrams, the white arrow is the applied load, and the black arrow is the resulting force in the filter. In the connected wall (above), the tension and compression in opposing sides of the wall resist one another. In the single wall (below), the surface is more likely to buckle,

In order to prevent the buckling of the filter, samples were heated without the axial force applied. Without the external force, however, bonding does not initiate between the filter and frit. The visualization of every channel on the top surface, therefore, cannot be accomplished because of the strength limitation of the filter thickness. It is possible that the method could be successful, given a filter with a greater wall thickness. However, in all filter geometries, the goal is to maximize flow area given an overall area constraint, so increasing the wall thickness is not optimal.

3.2 Temperature Cycles

Similar to how change in surface area type affected bonding, the temperature cycle undergone by the samples also drove process quality. The three different methods described in the method section 2.1 describe both the process temperatures and the heating or cooling rates. Preliminary research and testing determined the minimum temperatures necessary for powder frit wetting and the optimal temperature cycle for the surface types. The selected cycle was followed for the method testing where success was quantified through bond strength measurements.

3.2.1 Cycle Results

Referring to the temperature cycles based on their labels in Tables 2.1, 2.2, and 2.3, the most optimal cycle was determined to be 2. Both cycles 2 and 3 were preferred over the cycle 1 because the bonding process was greatly improved through the addition of an annealing cooling process. Additionally, little to no differences were found in the results between cycles 2 and 3; therefore, the additional 20 minutes of process soaking only added additional time to the cycle. The extra time at the peak temperature also increases the likelihood of devitrification, as described in section 3.2.2. The preferred cycle is reprinted in Table 3.1, and the furnace temperature, measured by a thermocouple, as a function of time is modeled in Figure 3.8.

Step	Rate (DPH)	Temperature (°C)	Hold (min)
1. Initial Heat / Process Soak	400	720	10
2. Rapid Cool / Anneal Soak	AFAP	480	30
3. Anneal Cool	100	370	0
4. Final Cool	AFAP	20	0

Table 3.1. The temperature cycle process deemed optimal in preliminary testing, and followed for method research of DPF to glass bonding.

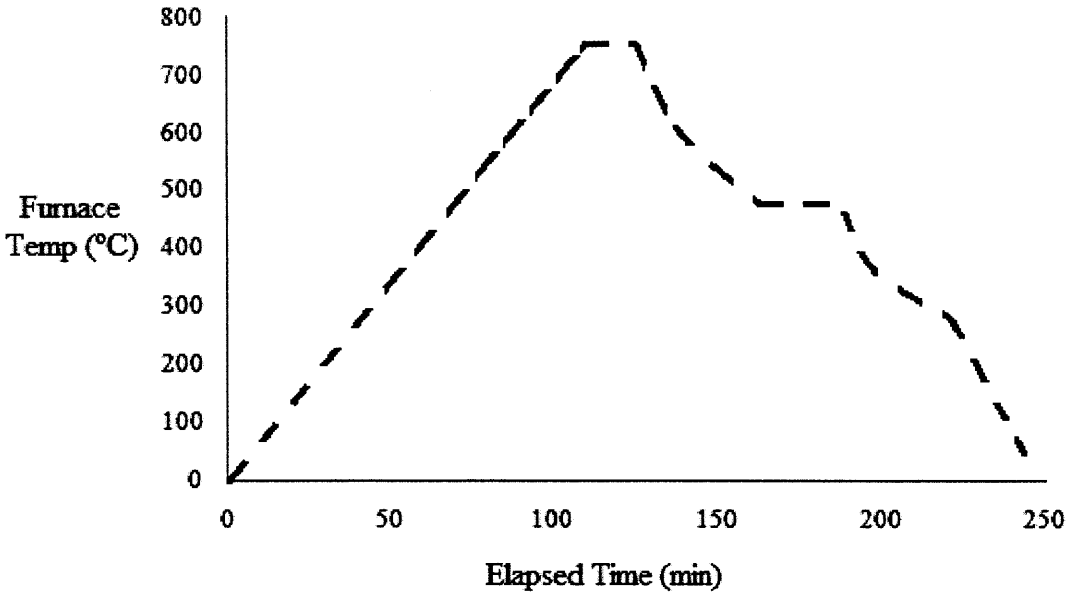

Figure 3.8. The model of the applied firing temperatures. Regions of interest include the process soak and annealing temperatures, where the temperature is held constant for several minutes.

3.2.2 Frit Properties

As the glass frit is heated, its physical characteristics soften and make bonding possible. At room temperature solid glass is described as a supercooled liquid, and increased temperature causes the viscosity to decrease and glass to behave more like a common liquid. The powder frit is initially a sand-like consistency and its large surface area reduces the glass transition temperature. Frit is made and sold in a range of different sizes, from powder to coarse grade, which is larger pieces of broken glass.

For a more efficient bonding process, the fine powder form of frit is preferred. As the frit is heated from a room temperature of 24°C to the tack fusing temperature of 720°C, surface temperature gradually overcomes gravity and the frit wets both surfaces. If the cooling rate is sufficiently slow, the glass will have time to consistently cover the surfaces and bond them together.

3.2.3 Silicon Carbide and fused quartz surface properties

Unlike the powder glass frit, the surface properties of the SiC DPF and SiO_2 layer do not undergo any phase or characteristic transitions. Multiple heating and cooling cycles of the SiC material does influence material properties because the temperatures in the method are below those necessary to melt SiC. Additionally, the filter maintains its high hardness, thermal conductivity, and strength during the process temperatures [ASM]. This makes sense because the tack bonding temperatures undergone by the samples are within the regeneration temperature range of the DPF in the use phase.

The fused quartz silicon dioxide layer is similar in atomic structure to the frit because the glass surface is also an amorphous structure. Because the properties and characteristics of the glass layer are not altered by the temperatures of the heating or regeneration cycles, fusible quartz and similar materials such as Vycor are ideal material choices for glass seal visualization windows.

4 CONCLUSION

Multiple variations of surface area types, powder frit applications, and temperature cycles were utilized to develop a visualization method of diesel particulate filters during PM trapping and regeneration. The hypothesized method was a development of previous source testing, with the addition of a bonding medium to examine more filter channels over a wider surface area [5]. The samples developed from the test methods were examined to determine the validity of powder frit bonding for SiC filter and fused quartz glass. An analysis of the samples provided the following conclusions:

- At temperatures in the range of diesel regeneration cycles, approximately 700°C, the characteristics of powder glass frit transform to that of a liquid. The transition of the frit from powder to liquid, then back to a solid form is analogous to that of lead-tin solder used to bond metals.

- Silicon carbide filter material is capable of being wetted with powder glass frit, adding further credence to the bonding method.
- Fused quartz glass and glasses with similar heat resistant properties, such as Vycor, are suitable visualization windows because they are unaffected by the temperature cycles of the bonding method and diesel emissions.
- Surfaces such as surface type B, where alternating channels are removed for viewing area, provide an adequate amount of surface area to facilitate bonding.
- Small surface areas that limit the number and length of channels are ideal for bonding. When the glass surface is under axial loading pressure, any surface inconsistencies cause unequal pressure concentrations and contribute to channel buckling. Additionally, the local height maxima diminish bond quality by increasing surface separation.
- The most prevalent failure modes of bonded samples are axial pressure and rotational motion perpendicular to the bond surface. Therefore, fixtures for holding bonded filter samples must prevent the filter from buckling and frit from shearing.

Further development of bonding techniques in tested methods are integral for research and innovations for future filter technologies. More efficient filters have a longer life cycle, limiting the number of replacements, and increasing the fuel economy. Given the widespread usage of diesel engines in manufacturing, industrial, and transportation applications, any emissions reduction will lead to significant air quality improvements.

4.1 Future Work

While the results of the present study did verify the validity of frit bonding for the DPF visualization method, they did not produce a sample with both sufficient bond strength and transparency. Therefore, further research with the aim of improving either or ideally both parameters will help improve the understanding of PM trapping and regeneration. The development of the present method is important because of the current research

aiming to maximize filter performance by altering geometry. Figure 4.1 displays filter cell patterns varying in size and shape.

In order to develop a useful comparison of filter properties for different geometries, the ideal visualization method must be applicable to various channel shapes. Additionally, emissions testing of a filter segment requires a specialized fixture to provide a viewing area and maintain bonding pressure. Emissions flow through the DPF section without the frit method sealed the glass to the filter using only pressure [5]. The combination of bonding frit and the fixture pressure is capable of providing a suitable seal for observation of the airtight emissions flow.

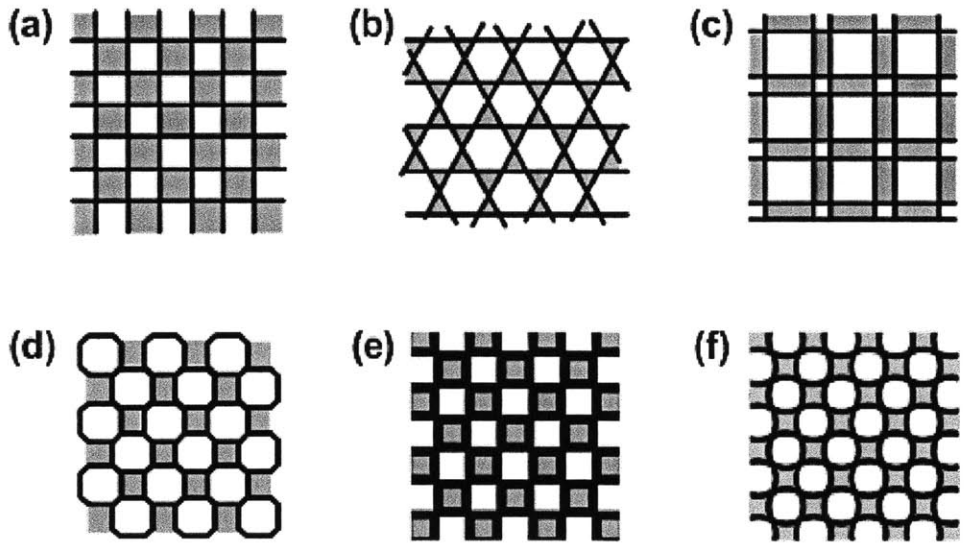

Figure 4.1. Various filter patterns and geometries of DPF channels.

Overall filter performance can be improved through different approaches; for example, an increase of filter working surface area, development of more efficient flow channels, or adapted regeneration cycles. Regardless of the improvement method, real-time examination of filter performance will increase the understanding and modeling of PM trapping and regeneration cycles and ultimately promote the development of better DPF's.

5 REFERENCES

[1] DieselNet Technology Guide, <http://www.dieselnet.com/tg.php>, 2011.

[2] Sappok, A., "The Nature of Lubricant- Derived Ash Related Emissions and Their Impact on Diesel After treatment System Performance," Massachusetts Institute of Technology, 2009.

[3] United States Environmental Protection Agency, <www.epa.gov/air/airpollutants.html>.

[4] Sappok, A, Wong, B., "Ash Effects on Diesel Particulate Filter Pressure Drop Sensitivity to Soot and Implications for Regeneration Frequency and DPF Control," SAE International Jounral of Fuels and Lubricants. 3.1 (2010).

[5] Cui, L, et al., "Microscopic Visualization of PM trapping and Regeneration in Micro-structural Pores on DPF wall," JSAE No. 370-20085302.

[6] ASM Handbook, "Engineering Tables: Ceramics and Glasses," ASM Handbooks Online, 2011.

[7] Bullseye Glass Co, "Heat & Glass," Tech Notes 4, <http://www.bullseyeglass.com/pdf/technotes_tipsheets/TechNotes_04.pdf>

[8] Heraeus Quarzglas, "Thermal Properties," <http://www.heraeus-quarzglas.de/en/quarzglas/thermalproperties/Thermal_properties.aspx>

6 APPENDIX

Sample Preparation

- Cut DPF section into sample size with abrasive saw and flood cooling
- Clean surfaces with alcohol and wipe away all liquids
- Establish level channel surface with diamond filing tool
- Apply thin layer of petroleum jelly to top surface of filter
- Stamp the lubricated surface lightly into a film of powder
- Remove any jelly or frit that was pushed between channels
- Apply cleaned quartz surface and fixture pressure for furnace heating